Polymer Testing 67 (2018) 450–456

Contents lists available at ScienceDirect

Polymer Testing

journal homepage: www.elsevier.com/locate/polytest

Morphological Raman analysis of short chain branched ethylene and propylene metallocenic copolymers

A.J. Satti[a,*], R. Quijada[b], J.M. Pastor[c], E.M. Vallés[d]

[a] Instituto de Química del Sur, INQUISUR, Universidad Nacional del Sur (UNS), 8000 Bahía Blanca, Argentina
[b] Departamento de Ingeniería Química, Fac. Ciencias Físicas y Matemáticas, Universidad de Chile, 2777 Santiago, Chile
[c] Departamento de Física de la Materia Condensada, Escuela de Ingenierías Industriales, Universidad de Valladolid, Paseo del Cauce 59, Valladolid 47011, Spain
[d] Planta Piloto de Ingeniería Química, PLAPIQUI, (UNS-CONICET) Camino "La Carrindanga", Km 7 - CC 717, 8000 Bahía Blanca, Argentina

ARTICLE INFO

Keywords:
Raman
Short chain branches
Polypropylene
Polyehtylene
Metallocenic
Olefin copolymers

ABSTRACT

Spectroscopic features in the Raman spectra of semicrystalline polyolefins that characterize different phase morphologies are reported. With growing incorporation of different 1-olefins, changes in the spectra due to different short chain branches are identified for polyethylene and polypropylene, both isotactic and syndiotactic. Bands were assigned to crystalline, semicrystalline and amorphous contents, and quantification was approached with the use of internal reference bands. The degree of crystallinity and the conformational order of the copolymers decrease with the increase in short chain branches content, and the behavior of larger short chains is different depending on the type of polymer analyzed. A semi ordered interphase was found, assigned and followed in all cases, as well as the evolution of amorphous phase with comonomer incorporation.

1. Introduction

Semicrystalline polymers have a heterogeneous microstructure consisting of crystalline and amorphous phases. Consequently, polymer properties are highly influenced by its crystalline morphology [1–19]. Other methods that provide quantitative measurements of the degree of crystallinity are available for the morphological characterization, as differential scanning calorimetry (DSC). The determination of crystallinity from this method is based on the assumption of a two-phase structure, which may indeed not be the case. Previous studies on semicrystalline polymers using vibrational spectroscopy have shown the existence of an intermediate transitional phase or interphase [1–6,20–36], consisting on semi-ordered, or short-range ordered systems that are frequent in polyolefins.

Raman spectroscopy is a fast and nondestructive method to probe the conformational states of the polymer chains. Thus, differentiation in the vibrational spectrum of chains in crystals with unique conformations must be expected [1,2,20–30,33–46]. Contents of different configurational and conformational states, order and length distribution of sequences can be potentially identified and related to chains in specific 'phases' [37–39].

For example, an interfacial region is present between crystalline lamellas and the amorphous phase of polyethylene (PE) and its short chain branched (SCB) copolymers. Mutter et al. [20] even split this interfacial region in interfacial crystal and liquid like components, which were thoroughly examined through free volume models [3–6]. Each of these phases was estimated through different bands, or their deconvolution, in the Raman spectrum [1,3–6,20,27–30,33–36]. Their intensities and positions depend on the degree of crystallinity of the sample [21,22]. Similar three phase morphologies with ordered helicoidal structures and sequences, exist in isotactic polypropylene (iPP) copolymers [2,24–26,42–45]. Still, there is not a common consensus on the estimation of each of the phases through Raman analysis. As long as known, neither there are studies involving copolymers of syndiotactic polypropylene (sPP), though it is known that the homopolymer also follows ordered helicoidal and all-trans structures, as well as an amorphous phase.

In this work we use Raman spectroscopy to characterize ethylene and propylene metallocenic copolymers. Metallocene catalysts made possible the synthesis of 1-olefin copolymers with well-defined structures, homogeneous comonomer composition, and narrow molecular weight distribution [1,5–14]. The introduction of a chosen 1-olefin during ethylene or propylene polymerization induces the insertion of SCB of a desired length. Comonomers of different length were used, in order to compare between different sizes of SCB in the morphologies. Also, both iso and syndio tacticities were taking into account for the propylene metallocenic copolymers. The effect of growing amounts of comonomer on the morphologies of all the polyolefins was studied.

* Corresponding author.
E-mail address: angel.satti@uns.edu.ar (A.J. Satti).

https://doi.org/10.1016/j.polymertesting.2018.03.036
Received 28 December 2017; Received in revised form 8 March 2018; Accepted 17 March 2018
Available online 20 March 2018

Table 1
Reaction conditions for the different syntheses.

Polymer	T (°C)	Stir (rad/s)	P (kPa)	Catalytic system	Reactor
PEX#	60	52	200	$[Et(Ind)_2]ZrCl_2$/MAO	Parr, 1 l
iPPX#	40	105	300	$[Me_2Si(2Me\text{-}Ind)_2]ZrCl_2$/MAO	Buchi, 1 l
sPPX#	55	105	200	$[Ph_2C(Flu)(Cp)]ZrCl_2$/MAO	Buchi, 1 l

2. Experimental

The syntheses of the polymers were carried in toluene for 30 min, under the conditions shown in Table 1. Polymerizations were then stopped with methanol acidified with HCl (2%). The resulting polymers were precipitated and then washed with methanol and acetone. Finally, the product was dried at room temperature. The tacticity and the amount of comonomer incorporated in the copolymers were measured by ^{13}C NMR at 90 °C using a Varian Inova 300 spectrometer operating at 75 Hz [1,7–10,12]. The nomenclature employed in this work to identify the copolymers is of the type PEX#, iPPX#, sPPX# where X and # are letters and numbers that identify, respectively, the comonomer used (H = 1-hexene, OD = 1-octadecene), and the approximate molar amount in percentage of comonomer incorporated to the polymer (Table 2).

The Raman spectra of the polymers were obtained on a confocal LabRam Dilor S.A. microspectrometer. The amount of crystalline, amorphous and interfacial polymer contents was determined from the analysis of the internal mode region of the Raman spectra (800 - 1550 cm^{-1}). The excitation source was a He/Ne laser (632.817 nm). The scattered light was collected by a microscope, followed by a notch filter. For deconvolution of the overlapping band systems, the curve analysis program Grams (supplied by Galactic Industries Corp.) was used. A combination of Gaussian and Lorenztian functions so as to give the best fit to the observed spectra was performed [2,28,34,35].

The thermal transitions were determined by differential scanning calorimetry (DSC), using a Perkin-Elmer Pyris 1 calorimeter under argon atmosphere and calibrated with indium and n-heptane standards. To ensure the same thermal history for all samples, the original and irradiated copolymers were first heated to 150 °C, maintained at 150 °C for two minutes, and then cooled down to 40 °C at 10 °C/min. After this treatment, the samples were reheated at 10 °C/min, and the corresponding endotherms were recorded between 40 and 150 at 10 °C/min. The melting peaks and the corresponding areas were determined to obtain the enthalpy (ΔH_f) of fusion. To estimate the degree of crystallinity (X_c) of the polymer, we used a ΔH_f value of 288 J/g for the melting enthalpy for 100% crystalline PE [47], and of 148 J/g for the melting enthalpy of 100% crystalline iPP [48].

Table 2
Monomer incorporation in the synthesized polymers.

Polymer	% comonomer
PE	–
PEH3	3.3
PEH9	9.2
PEH16	16.1
PEOD5	4.8
PEOD7	6.8
iPP	–
iPPH4	3.7
iPPH9	9.2
iPPOD3	3.0
sPP	–
sPPH3	3.1
sPPH16	16.1
sPPOD6	6.1

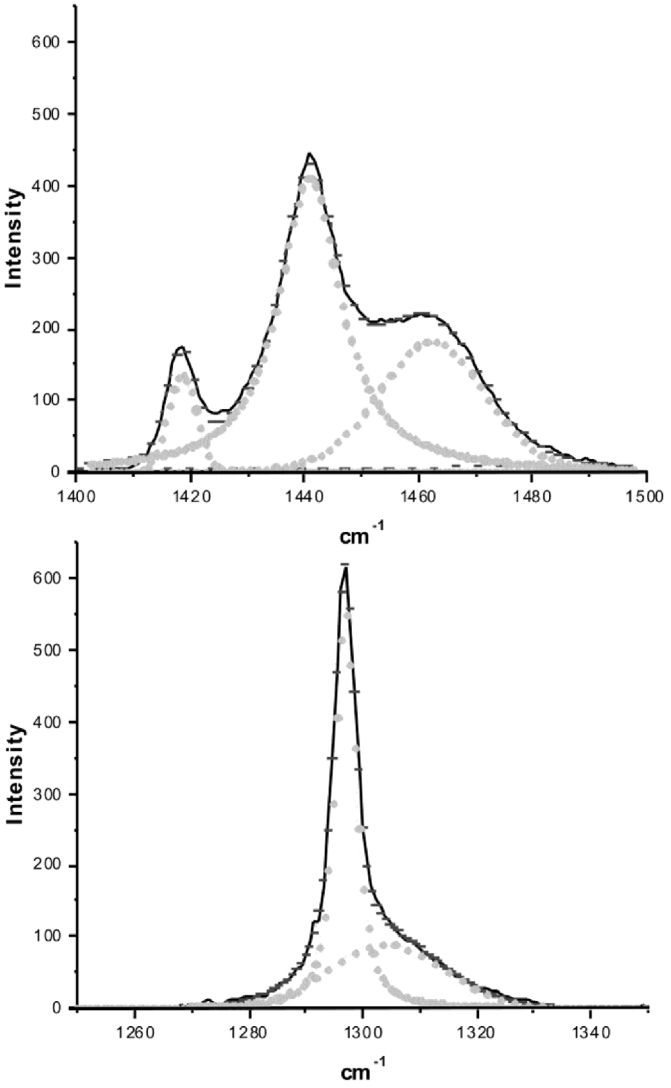

Fig. 1. Deconvolution of PEH3. Black solid line represents the original spectra, while the grey dashed line, the deconvolution adjustment. Dotted bands represent the respective deconvoluted bands at 1298 cm^{-1}, 1304 cm^{-1}, 1419 cm^{-1},1440 cm^{-1} and 1460 cm^{-1}.

3. Results and discussion

3.1. Ethylene copolymers

To quantitatively evaluate the phase structures of the PE polymers, we analyzed their Raman CH_2 twisting and bending internal regions. The mass fractions of the three PE phases, namely, the orthorhombic crystalline phase, the liquid-like amorphous phase, and the disordered anisotropic interfacial phase are calculated from the measured integrated intensities of three bands. They are: a) CH_2 bending band at 1419 cm^{-1} which is due to the crystalline portions alone, b) CH_2 twisting band located between 1303 and 1307 cm^{-1} belonging to the amorphous phase and c) another component of the same mode at 1298 cm^{-1} which can be attributed to both the crystalline phase and the interphase [27]. Fig. 1a shows the curve analysis performed on the polyethylene samples for the twisting at 1250 to 1350 cm^{-1} region while Fig. 1b does the same for the 1400 to 1500 cm^{-1} bending region. According to Strobl and Hagedorn [27], the total integrated intensity in the twisting region between 1250 cm^{-1} and 1350 cm^{-1}, I_t, is independent of the chain conformation, i.e. the amorphous and crystalline content. It therefore provides an internal intensity standard. The amorphous content, α_a (i.e. the mass fraction of the amorphous

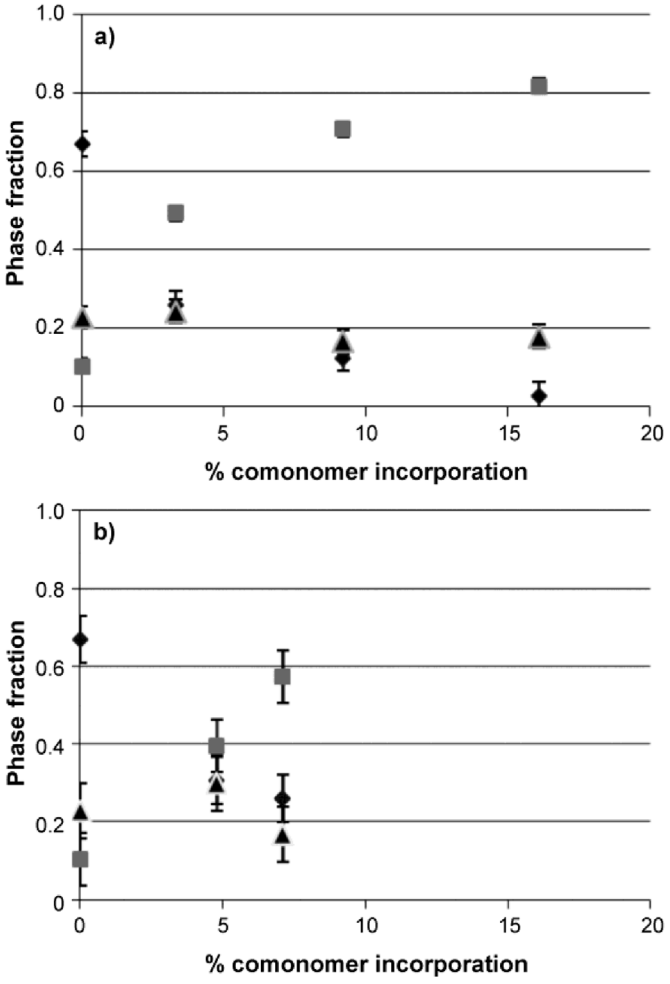

Fig. 2. Phase fraction in PEH (a) and POD (b) as a function of comonomer incorporation. Parameters α_c, α_a, and α_b are represented by ◆, ■, and ▲, respectively.

material), is then calculated by using the twisting bands (subscript t) simply as $\alpha_a = I_{1304}/I_t$. The crystalline content, α_c, is proportional to the intensity of the 1419 cm^{-1} band [28]; $\alpha_c = I_{1419}/(0.47 \times I_t)$. The constant 0.47 was experimentally determined from the spectra of fully crystalline PE [27,29,30]. This band is located in the CH_2 bending modes between 1400 and 1500 cm^{-1}. Finally, the interfacial content can be obtained as $\alpha_b = 1 - \alpha_a - \alpha_c$.

The analysis of the Raman spectra for the different PE copolymers is shown in Fig. 2 and it indicates a decrease in α_c and an increase of α_a as the comonomer incorporation increases, while the interfacial phase remained fairly constant. The interfacial content of the homopolymer is in accordance with the literature at around 20% [4,49]. Then, the interfacial phase did not exceed 25% of the total composition. Similar results were reported in the literature for random 1-butene, 1-hexene, and 1-octene PE copolymers [36], suggesting that a saturation value is reached for α_b when the comonomer incorporation becomes higher than about 6 mol %. At those concentrations of comonomer, the lamellar crystallite structure is lost and very small crystallites are formed under the conditions employed [1].

PEH9 and PEOD7 have similar crystallinity obtained from DSC (28 and 31% respectively) [11]. However, the parameter α_c obtained through Raman is different for both copolymers. The vibrational technique indicates that PEOD7 have higher crystallinity and similar interfacial content, consequently, lower amorphous content than PEH 9.

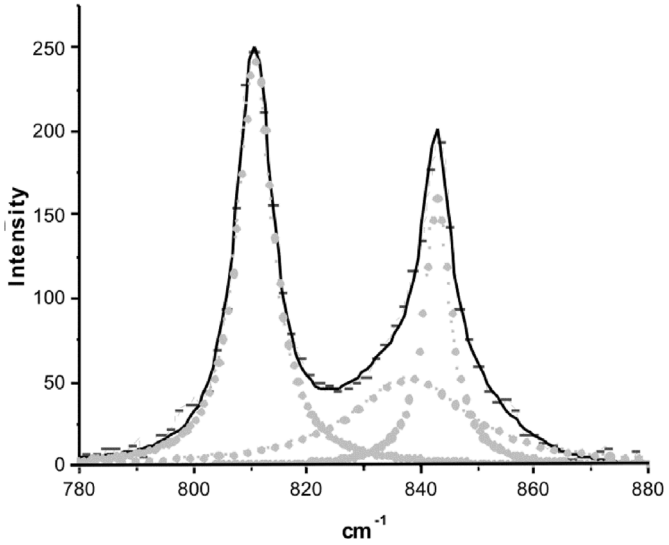

Fig. 3. Deconvolution of iPPH4. Black solid line represents the original spectra, while the grey dashed line, the deconvolution adjustment. Dotted bands represent the respective deconvoluted bands at 809 cm^{-1}, 836 cm^{-1}, and 840 cm^{-1}.

3.2. Isotactic propylene copolymers

The Raman analysis for crystalline and amorphous phases in iPP is usually focused in the region at 780-880 cm^{-1} [2,11,24–26,37–40,42–46], that mostly correlate with CH_2 rocking, and some C-C stretching. The peak at 809 cm^{-1} is associated to CH_2 rocking, entangled with the skeletical mode of symmetric stretching. It can be related to the crystalline order of a trans-gauche sequence in helicoidal conformation, with a propylene monomer sequence, $(CH_2CHCH_3)_n$, of at least, n = 15. The 840 cm^{-1} band is assigned to the rocking of CH_2 without being entangled to other modes, and it can be refered to helicoidal chains of at least n = 13, but with isomeric defects [2,50–52]. Thus, some authors assign this peak to some short range order semicrystalline phase of the iPP, also called as a crystal-amorphous transition phase [2,24–26]. Nielsen [2] proposes another peak near 830 cm^{-1}, assigned to chains with non helicoidal conformation. Moreover, taking into account this third assignation, a better deconvolution of these peaks contained in the abovementioned region can be obtained (Fig. 3). Then, a three phase structure can also be designed for iPP, and its copolymers.

In order to obtain referenced values of these peaks and thus obtain comparable values of the three phases, authors assigned different internal references. The band at 973 cm^{-1} corresponding to the vibrations of the sequences of isotactic segments in the helical conformation with minimal length n of 2–4 [37–39], is the mostly used as a reference band. It remains invariant even in the molten polymer [44–46,53].

Fig. 4 shows the spectra of iPP polymers, normalized under the reference peak at 973 cm^{-1}. Some works used the area below the region 780-880 cm^{-1} as an internal reference for iPP homopolymer, since it remained almost invariant comparing it to the 973 cm^{-1} band [2,46]. Looking to the figure, this might not be the case for the isotactic metallocenic copolymers since it can be clearly seen that the region 780-880 cm^{-1} seems to decrease with a constant 973 cm^{-1} peak. Thus, is preferred to work with the original reference band at 973 cm^{-1}. This band, along with the others around 809, 840, 898, 998 cm^{-1}, are associated with helical chain structures [30,38,39,53,54] of different order of “n” sequences of methylene. A significant reduction in the intensities of almost all of them is observed, being it more notorius in the peaks 840 (n > 13) and 998 (n > 5–10), as the incorporation of comonomer increases. It is worth to mention that the peak at 998 cm^{-1} was also related to cristallinity in other works [24,25], and the one at 840 cm^{-1} to semicristallinity as discussed above.

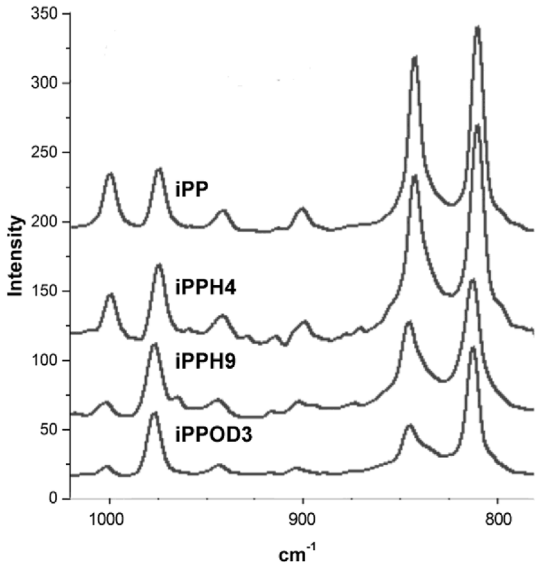

Fig. 4. Raman spectra of the isotactic propylene copolymers.

The decrease of those peaks might be related to the fact that as more comonomer is inserted, there is a lower proportion of consecutive propylene units. These two bands were also found to decrease in iPP copolymers analyzed by Prokhorov et al. [37], without significant difference between comonomers up to 1-octene (six carbon SCB). However, in this work, the copolymer with 1-octadecene (sixteen carbon SCB) definetely marks a difference in those bands if compared to one with similar incorporation of 1-hexene (four carbon SCB), as can be directly seen in Fig. 4. A logic reason is that, in proportion, there will be a higher reduction in propylene units when comparing the two copolymers. Evenmore, if calculated, the fraction of propylene units in iPPOD3 is much more similar to that of iPPH9 than to iPPH4. That explains the similarity between iPPH9 and iPPOD3 spectra.

Table 3 shows the normalized values obtained at the peaks of 809, and 840 cm^{-1}, after making the deconvolution of the area defined by the 780-880 cm^{-1} region. The table has also an extra column reporting the values obtained by DSC for cristallyne fraction. It can be clearly seen that the intensity values obtained for the peak at 809 cm^{-1} are lowered as the comonomer increase. However, it doesn't seem to have the same decay of X_c that was observed for DSC. On the other side, the crystalline decrease for each copolymer can be better approached to that obtained with DSC, if the contribution of both peaks, I_{809} and I_{840}, is taking into account. This might be better obseved in Fig. 5, where al DSC cristallinity fractions where normalized to that of iPP, which has the higher crystallinity and no comonomer content. There, the values I_{809}/I_{973} and $(I_{809}+ I_{840})/I_{973}$ were also normalized to those for the iPP homopolymer. In the graph, it can be seen that each point related to $(I_{809}+ I_{840})/I_{973}$ is nearer than those of I_{809}/I_{973}, to the DSC values. This means that for these copolymers, as most authors designate, the peak at 840 cm^{-1} might also be assigned to a certain semicristallinity, mainly, the one with defects due to the incorporation of lateral chains. Neway et al. [5] and Lagaron et al. [23] also found that DSC results correlated better with the sum of both pure crystals and small defective crystals with lateral disorder, but for ethylene – 1-octene copolymers.

Table 3
Relative intensities of bands.

	I_{809}/I_{973}	I_{840}/I_{973}	$(I_{809}+ I_{840})/I_{973}$	X_c (%)
iPP	3.46	3.09	6.55	70.9
iPPH4	2.90	1.65	4.55	37.8
iPPH9	1.65	0.525	2.18	16.9
iPPOD3	2.09	0.536	2.63	36.1

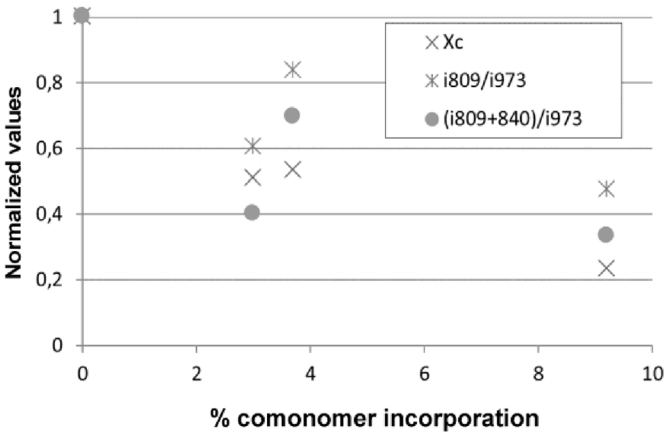

Fig. 5. Normalized values of the Raman relative intensities and DSC X_c, to those of iPP.

Nevertheless, one important thing to mention, is that the comparisson is being made by both techniques reaching room temperature. That means that the DSC crystallinity at room temperature requires truncation of the melting peak area, thus some error involved by this technique.

3.3. Syndiotactic propylene copolymers

IR absorbance [55–58] and Raman scattering [50,59] have been used to identify the presence of (gauche–gauche–trans– trans), $(ggtt)_n$, helical and all-trans, $(tttt)_n$, planar zigzag conformed chains in sPP [50,60–65]. However, up to date, there are no works concerning the Raman analysis of short chain branched copolymers of syndiotactic polypropylene.

The ability to synthesize, and thus to study experimentally, highly stereoregular sPP and its SCB copolymers was only realized around 1990 with the advent of metallocene catalysts [8,9,66,67]. So, in this work, the conformations of sPP are followed with the incorporation of the 1-olefin comonomers in well defined metallocenic copolymers. For the spectroscopic analysis, an internal reference around 1157 cm^{-1} was used. This peak had been identified as insensitive to polypropylene configuration and conformation [60,61]. As it simply confirms the presence of polypropylene, is often used as a normalization factor for other peaks [60]. After normalization, the spectra of Fig. 6 were obtained.

As for iPP, the region between 790 and 890 cm^{-1} shows the combination of three CH_2 rocking bands that are sensitive to helical, amorphous, and trans planar zigzag content, at 826, 845, and 865 cm^{-1}, respectively. These bands can relatively quantify the content of each phase [60,62]. Indeed, the area below this region remains invariant, when normalized with the peak at 1157 cm^{-1}, between the copolymers. This was confirmed after deconvolution of this region (Fig. 7), and then observing a similar tendency for each phase as the incorporation of comonomer grew in the copolymers (Fig. 8) for both, 1157 and 790-890 cm^{-1}, normalization. The tendency was followed for

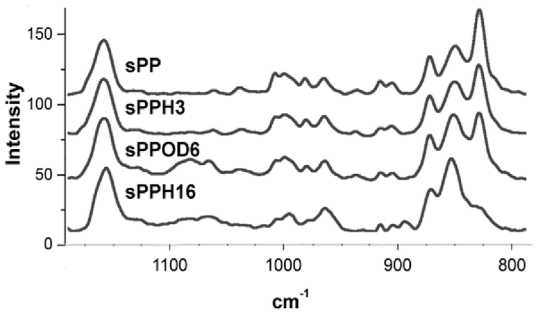

Fig. 6. Raman spectra of the syndiotactic propylene copolymers.

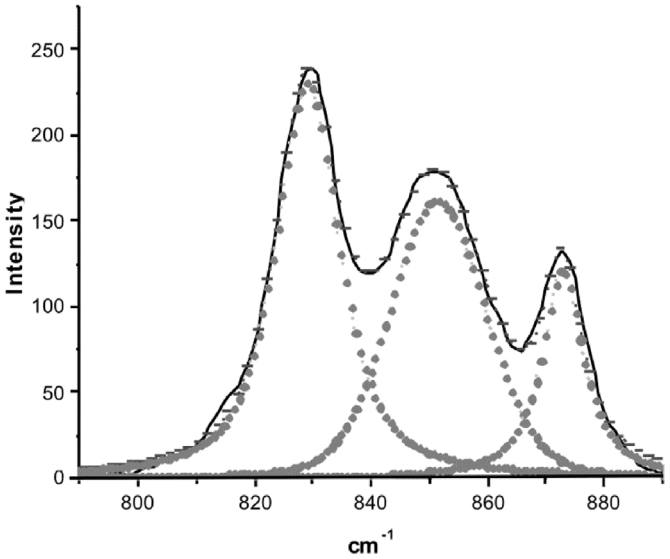

Fig. 7. Deconvolution of sPPH3. Black solid line represents the original spectra, while the grey dashed line the deconvolution adjustment. Dotted bands represent the respective deconvoluted bands around 826 cm^{-1}, 845 cm^{-1}, and 865 cm^{-1}.

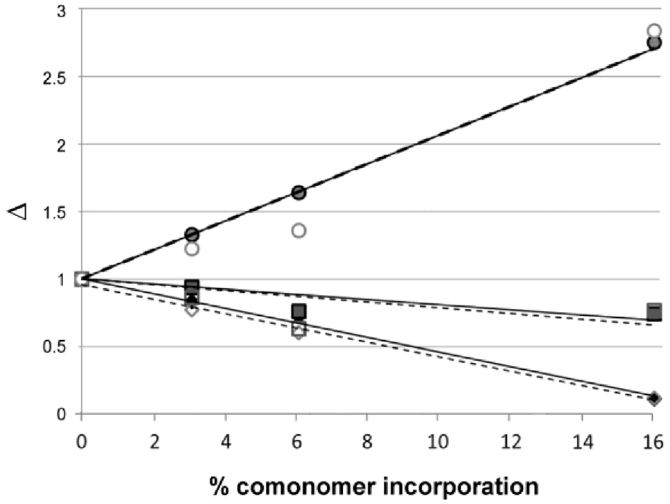

Fig. 8. Phase tendencies by comonomer incorporation. Bold lines and symbols correspond to normalizations made with the area of the region 790-890 cm^{-1} as reference. Dashed lines and hollow symbols correspond to normalizations made with the area of the 1157 cm^{-1} band as reference. Circles, squares and romboids were used for the calculation of amorphous, trans, and helicoidal phases respectively.

the ratio of the respective normalized band area (nBA) of each copolymer (cop), to that of the normalized homopolymer (sPP) ($\Delta = nBA_{cop}/nBA_{sPP}$). Normalized band areas were calculated for amorphous, trans and helicoidal phases (subscripts a, t and h, respectively), as for example $nBA_a = BA_a/BA_{790\text{-}890}$ or $nBA_a = BA_a/BA_{1157}$, depending on the area used as reference.

Then, quantification was approached by simply using the values of the fractions nBA_a, nBA_t and nBA_h calculated with the area deduced in the 790-890 cm^{-1} region. Therefore, phase contents of each ordered structure and the amorphous phase are shown in Fig. 9. There, it can be seen that the helicoidal structure decreases almost linearly with comonomer incoporation. Note that the 6,1% corresponds to 1-octadecene, while the other points to 1-hexene, though no differentiation seem to be evident in the tendencies. To this decay follows an opposite but similar tendency to increase in the amorphous content, and a little decrease of the all trans conformation. It is evident that the defects induced with the incorporation of short chain branches affects much

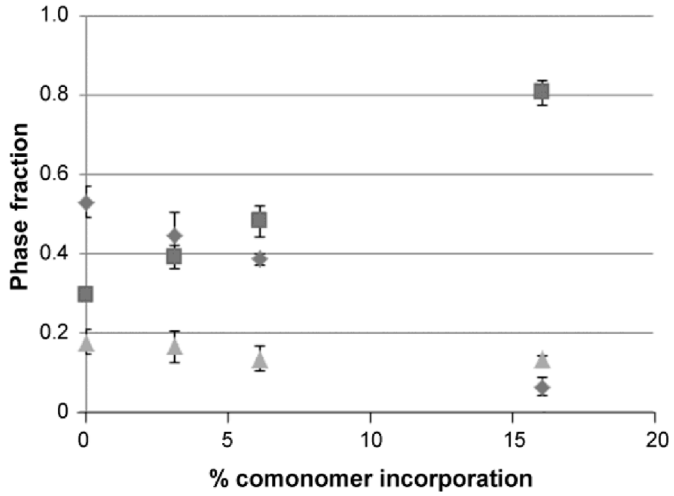

Fig. 9. Phase fraction in sPP copolymers as a function of comonomer incorporation. Fractions nBA_h, nBA_t, and nBA_a are represented by ◆, ▲, and ■, respectively.

more the three dimensional sequence of the helicoidal structure than the trans planar zig zag of the polypropylene main chain.

4. Conclusions

The role of short chain branches of four and sixteen carbons on the morphology of well-defined ethylene and propylene metallocenic polyolefines, through incorporation of different comonomers, has been studied by means of fast and non-destructive vibrational Raman spectroscopy. Morphologies of these copolymers were practically defined within three phases; crystalline, amorphous and a semicrystalline interphase. Changes could be found in the Raman spectra that are related with the increase of content in the incorporated comonomer, mainly causing the alteration of the degree of crystallinity and the conformational composition of the polymers.

Morphologic analysis for the spectra of the ethylene copolymers, can be followed through the deconvoluted bands of 1304 and 1419 cm^{-1}, in the bending and twisting CH_2 region, referred to amorphous and crystalline content respectively, after whom the interphase content can be deduced. Results indicated a rapid decay in crystallinity with comonomer incorporation, with a correspondent increase of the amorphous phase and practically constant interphase content around 20%. For the copolymer with 1-octadecene, crystallinity seemed to be higher than that for a copolymer with a similar content of 1-hexene, thus, minor SCB.

Three different conformational states can be identified for iPP copolymers, and deconvoluted in three bands under the CH_2 rocking region at 780-880 cm^{-1}. Chains in regular helical conformation present in crystals and related to the intensity of the 808 cm^{-1} band, chains in helical conformation with defects and certain short order related to the intensity of the 840 cm^{-1} band and an amorphous phase related to the intensity of the 836 cm^{-1} band. The short range order band at 840 cm^{-1} was more affected for the 1-octadecene SCB copolymer, when compared to the copolymer with similar molar incorporation of 1-hexene, due to a lower proportion of propylene units in the former.

Raman analysis of syndiotactic copolymers could also be performed, seemingly for the first time. The content of ordered helicoidal, amorphous and all-trans conformations were deconvoluted from an area at the 790-890 cm^{-1} CH_2 rocking region, to the peaks at 826, 845 and 865 cm^{-1} respectively. This area was confirmed as internal standard, as it stood invariant under the normalization with the well-known internal reference band at 1157 cm^{-1}, which is insensitive to propylene configuration and conformation. Therefore, contents for the different conformations were revealed for the syndiotactic polymers. Helicoidal

content decreased with a similar tendency than the corresponding amorphous content increase. Thus, the all-trans conformation presented a considerable smaller decay. No differences between different SCB copolymers could be stated for this case.

Aknowledgements

The authors wish to thank Universidad Nacional del Sur (PGI UNS 24) and CONICET (Argentina) (PIP 5836), Universidad de Chile, Universidad de Valladolid (Spain) and specially Project CYTED VIII. 11 (unesco 331210) for supporting this work.

References

[1] A.J. Satti, N.A. Andreucetti, R. Quijada, C. Sarmoria, J.M. Pastor, E.M. Vallés, Gamma-irradiated metallocenic polyethylene and ethylene-1-hexene copolymers, J. Appl. Polym. Sci. 117 (2010) 290–301, http://dx.doi.org/10.1002/app.31983.
[2] A. Nielsen, D. Batchelder, R. Pyrz, Estimation of crystallinity of isotactic polypropylene using Raman spectroscopy, Polymer 43 (2002) 2671–2676, http://dx.doi.org/10.1016/S0032-3861(02)00053-8.
[3] M. Hedenqvist, A. Angelstok, L. Edsberg, T. Larsson, U.W. Gedde, Diffusion of small-molecule penetrants in polyethylene: free volume and morphology, Polymer 37 (1996) 2887–2902.
[4] B. Neway, M.S. Hedenqvist, U.W. Gedde, Effect of thermal history on free volume and transport properties of high molar mass polyethylene, Polymer 44 (2003) 4003–4009.
[5] B. Neway, Å. Westberg, A. Mattozzi, M.S. Hedenqvist, M. Giacinti Baschetti, V.B.F. Mathot, U.W. Gedde, Free volume and transport properties of homogeneous poly(ethylene-co-octene)s, Polymer 45 (2004) 3913–3922.
[6] A. Mattozzi, B. Neway, M.S. Hedenqvist, U.W. Gedde, Morphological interpretation of n-hexane diffusion in polyethylene, Polymer 46 (2005) 929–938.
[7] A.G. Simanke, G.B. Galland, L. Freitas, J.A.H. da Jornada, R. Quijada, R.S. Mauler, Influence of the comonomer content on the thermal and dynamic mechanical properties of metallocene ethylene/1-octene copolymers, Polymer 40 (1999) 5489–5495, http://dx.doi.org/10.1016/S0032-3861(98)00771-X.
[8] R. Quijada, J.L. Guevara, G.B. Galland, F.M. Rabagliati, J.M. Lopez-Majada, Synthesis and properties coming from the copolymerization of propene with α-olefins using different metallocene catalysts, Polymer 46 (2005) 1567–1574, http://dx.doi.org/10.1016/J.POLYMER.2004.11.115.
[9] J.M. López-Majada, H. Palza, J.L. Guevara, R. Quijada, M.C. Martínez, R. Benavente, J.M. Pereña, E. Pérez, M.L. Cerrada, Metallocene copolymers of propene and 1-hexene: the influence of the comonomer content and thermal history on the structure and mechanical properties, J. Polym. Sci. Part B Polym. Phys. 44 (2006) 1253–1267, http://dx.doi.org/10.1002/polb.20781.
[10] H. Palza, J.M. López-Majada, R. Quijada, R. Benavente, E. Pérez, M.L. Cerrada, Metallocenic copolymers of isotactic propylene and 1-octadecene: crystalline structure and mechanical behavior, Macromol. Chem. Phys. 206 (2005) 1221–1230, http://dx.doi.org/10.1002/macp.200500036.
[11] A.J. Satti, N.A. Andreucetti, R. Quijada, C. Sarmoria, E.M. Vallés, Effect of DBPH and vacuum gamma radiation on metallocenic ethylene-1-hexene and ethylene-1-octadecene copolymers, Radiat. Phys. Chem. 79 (2010) 9–15, http://dx.doi.org/10.1016/j.radphyschem.2009.08.008.
[12] A.J. Satti, N.A. Andreucetti, R. Quijada, E.M. Vallés, Crosslinking of metallocenic α-olefin propylene copolymers by vacuum gamma irradiation, Radiat. Phys. Chem. 81 (2012) 1874–1880, http://dx.doi.org/10.1016/J.RADPHYSCHEM.2012.07.007.
[13] A.J. Satti, N.A. Andreucetti, E.M. Vallés, J.M. Carella, C.J. Pérez, Use of SSA to detect structural changes in metallocenic ethylene/α-olefin copolymers and their free radical post-reactor modifications, Polym. Degrad. Stab. 125 (2016) 43–48, http://dx.doi.org/10.1016/J.POLYMDEGRADSTAB.2016.01.001.
[14] A.J. Satti, E.C. Molinari, A.G.O. de Freitas, W.R. Tuckart, C. Giacomelli, A.E. Ciolino, E.M. Vallés, Improvement in abrasive wear resistance of metallocenic polypropylenes by adding siloxane based polymers, Mater. Chem. Phys. 188 (2017) 100–108, http://dx.doi.org/10.1016/J.MATCHEMPHYS.2016.12.007.
[15] P. Colomban, J.M. Herrera Ramirez, R. Paquin, A. Marcellan, A. Bunsell, Micro-Raman study of the fatigue and fracture behaviour of single PA66 fibres: comparison with single PET and PP fibres, Eng. Fract. Mech. 73 (2006) 2463–2475, http://dx.doi.org/10.1016/J.ENGFRACMECH.2006.04.033.
[16] S. Humbert, O. Lame, R. Séguéla, G. Vigier, A re-examination of the elastic modulus dependence on crystallinity in semi-crystalline polymers, Polymer 52 (2011) 4899–4909, http://dx.doi.org/10.1016/J.POLYMER.2011.07.060.
[17] Y. Gao, M. Xie, L. Liu, J. Li, J. Kuang, W. Ma, W. Zhou, S. Xie, Z. Zhang, Effect of supra-molecular microstructures on the adhesion of SWCNT fiber/iPP interface, Polymer 54 (2013) 456–463, http://dx.doi.org/10.1016/J.POLYMER.2012.11.043.
[18] M. Cocca, R. Androsch, M.C. Righetti, M. Malinconico, M.L. Di Lorenzo, Conformationally disordered crystals and their influence on material properties: the cases of isotactic polypropylene, isotactic poly(1-butene), and poly(l-lactic acid), J. Mol. Struct. 1078 (2014) 114–132, http://dx.doi.org/10.1016/J.MOLSTRUC.2014.02.038.
[19] L. Mandelkern, Crystallization of Polymers, McGraw-Hill, New York, 1964.
[20] R. Mutter, W. Stille, G. Strobl, Transition regions and surface melting in partially crystalline polyethylene: a Raman spectroscopic study, J. Polym. Sci. Part B Polym. Phys. 31 (1993) 99–105, http://dx.doi.org/10.1002/polb.1993.090310113.
[21] J.M. Lagaron, On the use of a Raman spectroscopy band to asses the crystalline lateral packing in polyethylene, J. Mater. Sci. 37 (2002) 4101–4107.
[22] J.M. Lagaron, The factor group splitting phenomenon: a vibrational spectroscopy approach to assess polymer crystallinity and crystalline density, Macromol. Symp. 184 (2002) 19–36.
[23] J. Lagaron, S. López-Quintana, J. Rodriguez-Cabello, J. Merino, J. Pastor, Polymer 41 (2000) 2999.
[24] M. Tanaka, R. Young, Molecular orientation distributions in the crystalline and amorphous regions of uniaxially oriented isotactic polypropylene films determined by polarized Raman spectroscopy, J. Macromol. Sci. Part B Phys. 44 (2005) 967–991, http://dx.doi.org/10.1080/00222340500323599.
[25] T. Kida, Y. Hiejima, K.H. Nitta, Molecular orientation behavior of isotactic polypropylene under uniaxial stretching by rheo-Raman spectroscopy, Express Polym. Lett. 10 (2016) 701–709, http://dx.doi.org/10.3144/expresspolymlett.2016.63.
[26] M. Arruebarrena de Báez, P. Hendra, M. Judkins, The Raman spectra of oriented isotactic polypropylene, Spectrochim. Acta Part A Mol. Biomol. Spectrosc. 51 (1995) 2117–2124, http://dx.doi.org/10.1016/0584-8539(95)01512-1.
[27] G.R. Strobl, W. Hagedorn, Raman spectroscopic method for determining the crystallinity of polyethylene, J. Polym. Sci. Polym. Phys. Ed. 16 (1978) 1181–1193, http://dx.doi.org/10.1002/pol.1978.180160704.
[28] D. Barron, C. Birkinshaw, Ultra-high molecular weight polyethylene – evidence for a three-phase morphology, Polymer (Guildf.) 49 (2008) 3111–3115, http://dx.doi.org/10.1016/J.POLYMER.2008.05.004.
[29] M. Glotin, R. Domszy, L. Mandelkern, A Raman-spectroscopic study of solution-crystallized polyethylenes, J. Polym. Sci. Polym. Phys. Ed. 21 (1983) 285–294, http://dx.doi.org/10.1002/pol.1983.180210210.
[30] G. Keresztury, E. Földes, On the Raman spectroscopic determination of phase distribution in polyethylene, Polym. Test. 9 (1990) 329–339, http://dx.doi.org/10.1016/0142-9418(90)90004-W.
[31] A. Boukenter, T. Achibat, E. Duval, G. Lorentz, Beautemp, Polym. Commun. 32 (1991) 258.
[32] G.R. Strobl, The Physics of Polymers : Concepts for Understanding Their Structures and Behavior, Springer, 2007.
[33] M. Failla, R.G. Alamo, L. Mandelkern, On the analysis of the Raman internal modes of crystalline polyethylene, Polym. Test. 11 (1992) 151–159.
[34] M. Glotin, L. Mandelkern, A Raman spectroscopic study of the morphological structure of the polyethylenes, Colloid Polym. Sci. 260 (1982) 182–192, http://dx.doi.org/10.1007/BF01465438.
[35] R.G. Alamo, L. Mandelkern, Thermodynamic and structural properties of ethylene copolymers, Macromolecules 22 (1989) 1273–1277, http://dx.doi.org/10.1021/ma00193a045.
[36] R.G. Alamo, B.D. Viers, L. Mandelkern, Phase structure of random ethylene copolymers: a study of counit content and molecular weight as independent variables, Macromolecules 26 (1993) 5740–5747, http://dx.doi.org/10.1021/ma00073a031.
[37] K.A. Prokhorov, G.Y. Nikolaeva, E.A. Sagitova, P.P. Pashinin, P.M. Nedorezova, A.N. Klyamkina, Regularity modes in Raman spectra of polyolefins: Part I. Propylene/olefin copolymers, Vib. Spectrosc. 85 (2016) 22–28, http://dx.doi.org/10.1016/J.VIBSPEC.2016.03.021.
[38] K. Chernyshov, D. Gen, Y. Shemouratov, K. Prokhorov, G. Nikolaeva, E. Sagitova, P. Pashinin, A. Kovalchuk, A. Klyamkina, P. Nedorezova, B. Shklyaruk, V. Optov, Raman structural study of copolymers of propylene with ethylene and high olefins, Macromol. Symp. 296 (2010) 505–516, http://dx.doi.org/10.1002/masy.201051067.
[39] G. Yu Nikolaeva, E.A. Sagitova, K.A. Prokhorov, P.P. Pashinin, P.M. Nedorezova, A.N. Klyamkina, M.A. Guseva, V.A. Gerasin, Using Raman spectroscopy to determine the structure of copolymers and polymer blends, Ser. J. Phys. Conf. Ser. 826 (2017), http://dx.doi.org/10.1088/1742-6596/755/1/011001.
[40] J.P. Tomba, C.D. Mana, C.J. Perez, P.M. Desimone, G.B. Galland, Microstructural characterization of semicrystalline copolymers by Raman spectroscopy, Polym. Test. 52 (2016) 71–78, http://dx.doi.org/10.1016/j.polymertesting.2016.04.001.
[41] P.J. Hendra, J. Vile, H.A. Willis, V. Zichy, M.E.A. Cudby, The effect of cooling rate upon the morphology of quenched melts of isotactic polypropylenes, Polymer 25 (1984) 785–790.
[42] H.N. Türkçü, Investigation of the Crystallinity and Orientation of Polypropylene with Respect to Temperature Changes Using FTIR, XRD, and Raman Techniques, Master Thesis Department of Chemistry, Bilkent University, 2004 Available from http://www.thesis.bilkent.edu.tr/0002621.pdf.
[43] J.M. Chalmers, H.G.M. Edwards, J.S. Lees, D.A. Long, M.W. Mackenzie, H.A. Willis, Raman spectra of polymorphs of isotactic polypropylene, J. Raman Spectrosc. 22 (1991) 613–618, http://dx.doi.org/10.1002/jrs.1250221104.
[44] E. Andreassen, Infrared and Raman spectroscopy of polypropylene, in: J. Karger-Kocsis (Ed.), Polypropylene. Polymer Science and Technology Series, vol. 2, Springer, Dordrecht, 1999, , http://dx.doi.org/10.1007/978-94-011-4421-6_46.
[45] T. Sundell, H. Fagerholm, H. Crozier, Isotacticity determination of polypropylene using FT-Raman spectroscopy, Polymer 37 (1996) 3227–3231.
[46] C. Minogianni, K.G. Gatos, C. Galiotis, Estimation of crystallinity in isotropic isotactic polypropylene with Raman spectroscopy, Appl. Spectrosc. 59 (2005) 1141–1147, http://dx.doi.org/10.1366/0003702055012681.
[47] F.M. Mirabella, A. Bafna, Determination of the crystallinity of polyethylene/?-olefin copolymers by thermal analysis: relationship of the heat of fusion of 100% polyethylene crystal and the density, J. Polym. Sci. Part B Polym. Phys. 40 (2002) 1637–1643, http://dx.doi.org/10.1002/polb.10228.
[48] J. (József) Karger-Kocsis, Polypropylene ;: Structure, Blends and Composites, Chapman & Hall, 1995.
[49] J. Cheng, M. Fone, V.N. Reddy, K.B. Schwartz, H.P. Fisher, B. Wunderlich,

Identification and quantitative analysis of the intermediate phase in a linear high-density polyethylene, J. Polym. Sci.: Polym. Phys. 32 (1994) 2683–2693.
[50] G. Masetti, F. Cabassi, G. Zerbi, Vibrational spectrum of syndiotactic polypropylene. Raman tacticity bands and local structures of iso- and syndiotactic polypropylenes, Polymer 21 (1980) 143–152, http://dx.doi.org/10.1016/0032-3861(80)90053-1.
[51] G.V. Fraser, P.J. Hendra, D.S. Watson, M.J. Gall, H.A. Willis, M.E.A. Cudby, The vibrational spectrum of polypropylene, Spectrochim. Acta Part A Mol. Spectrosc. 29 (1973) 1525–1533, http://dx.doi.org/10.1016/0584-8539(73)80216-8.
[52] M.I. Ize-Lyamu, Disorder in the molecular conformation of crystalline isotactic polypropylene at high pressures, Mat. Res. Bull. (1983) 18,225–18,229.
[53] H. Tadokoro, M. Kobayashi, M. Ukita, K. Yasufuku, S. Murahashi, T. Torii, Normal vibrations of the polymer molecules of helical conformation. V. Isotactic polypropylene and its deuteroderivatives, J. Chem. Phys. 42 (1965) 1432–1449, http://dx.doi.org/10.1063/1.1696134.
[54] R.G. Snyder, J.H. Schachtschneider, Valence force calculation of the vibrational spectra of crystalline isotactic polypropylene and some deuterated polypropylenes, Spectrochim. Acta 20 (1964) 853–869, http://dx.doi.org/10.1016/0371-1951(64)80084-9.
[55] T. Nakaoki, T. Yamanaka, Y. Ohira, F. Horii, Dynamic FT-IR analysis of the crystallization to the planar zigzag form for syndiotactic polypropylene, Macromolecules 33 (2000) 2718–2721, http://dx.doi.org/10.1021/MA9915428.
[56] L. Guadagno, L. D'Arienzo, V. Vittoria, Correlation between crystallinity and some infrared bands in the spectra of syndiotactic poly(propylene), Macromol. Chem. Phys. 201 (2000) 246–250.
[57] T. Ishioka, N. Masaoka, Normal mode analysis of syndiotactic polypropylene (T2G2T6G2) form, Polymer 43 (2002) 4639–4644, http://dx.doi.org/10.1016/S0032-3861(02)00273-2.
[58] V. Gregoriou, G. Kandilioti, K. Gatos, An infrared spectroscopic approach to the polymorphic behavior of syndiotactic polypropylene and its crystal–crystal transformations during mechanical stretching, Vib. Spectrosc. 34 (2004) 47–53, http://dx.doi.org/10.1016/J.VIBSPEC.2003.08.004.
[59] J. Jin, H. Lim, S.S. Kim, K. Song, Polarized Raman spectroscopic studies of syndiotactic polypropylene, Polymer (Korea) 26 (2002) 745–751.
[60] M.S. Sevegney, R.M. Kannan, A.R. Siedle, R. Naik, V.M. Naik, Vibrational spectroscopic investigation of stereoregularity effects on syndiotactic polypropylene structure and morphology, Vib. Spectrosc. 40 (2006) 246–256, http://dx.doi.org/10.1016/J.VIBSPEC.2005.10.003.
[61] J.L. Koenig, L.E. Wolfram, J.G. Grasselli, Infrared measurement of configuration and stereoregularity in polymers—II. Application to syndiotactic polypropylene, Spectrochim. Acta 22 (1966) 1233–1242, http://dx.doi.org/10.1016/0371-1951(66)80026-7.
[62] T. Hahn, W. Suen, S. Kang, S. Hsu, H. Stidham, A. Siedle, An analysis of the Raman spectrum of syndiotactic polypropylene. 1. Conformational defects, Polymer (Guildf) 42 (2001) 5813–5822, http://dx.doi.org/10.1016/S0032-3861(00)00904-6.
[63] J.M. Chalmers, Laser-Raman spectrum of helical syndiotactic polypropylene, Polymer 18 (1977) 681–684, http://dx.doi.org/10.1016/0032-3861(77)90235-X.
[64] Shaw Ling Hsu, Thomas Hahn, Wu Suen, Shuhui Kang, H.D. Stidham, A.R. Siedle, An analysis of Raman spectra of syndiotactic polypropylenes. 2. Configurational defects, Macromolecules 34 (2001) 3376–3383, http://dx.doi.org/10.1021/MA001448N.
[65] K.G. Gatos, G. Kandilioti, C. Galiotis, V.G. Gregoriou, Mechanically and thermally induced chain conformational transformations between helical form I and transplanar form III in syndiotactic polypropylene using FT-IR and Raman spectroscopic techniques, Polymer 45 (2004) 4453–4464, http://dx.doi.org/10.1016/J.POLYMER.2004.03.095.
[66] J.A. Ewen, R.L. Jones, A. Razavi, J.D. Ferrara, Syndiospecific propylene polymerizations with Group IVB metallocenes, J. Am. Chem. Soc. 110 (1988) 6255–6256, http://dx.doi.org/10.1021/ja00226a056.
[67] P. Longo, A. Proto, A. Grassi, P. Ammendola, Stereospecific polymerization of propylene in the presence of homogeneous catalysts: ligand-monomer enantioselective interactions, Macromolecules 24 (1991) 4624–4625, http://dx.doi.org/10.1021/ma00016a024.